PHYSICAL REVIEW B VOLUME 43, NUMBER 9 15 MARCH 1991-II

Surface conductance and the diffusion of H and D in Pd

G. L. Powell
Oak Ridge Y-12 Plant, Martin Marietta Energy Systems, Inc., Oak Ridge, Tennessee 37831-8096

J. R. Kirkpatrick
Computing and Telecommunications Division, Martin Marietta Energy Systems, Inc., Oak Ridge, Tennessee 37831-7039

(Received 27 August 1990)

The absorption of H and D into a palladium sphere of precise radius and density is examined experimentally with use of pressure-volume-temperature measurements and control techniques to achieve the stepwise boundary condition and constant pressure assumed in the common solutions to Fick's second law. Measurements were made at temperatures over the range of 298 to 1373 K after preparing the Pd by cyclic baking of the sphere in vacuum and in very pure H_2 or D_2. Near 473 K and higher temperatures, excellent agreement with Fick's-second-law solutions were obtained. Below 473 K, deviations from simple diffusion in the metal were observed and explained by postulating a surface conductance. From known solutions for diffusion in a sphere with a surface conductance, the diffusion coefficients (D) and the minimum achievable surface conductances (h) were determined to be $D_{\mathrm{H}}=3.512\times10^{-7}e^{-(2759.9\ \mathrm{K})/T}\ \mathrm{m^2\,s^{-1}}$, $D_{\mathrm{D}}=2.219\times10^{-7}e^{-(2538.0\ \mathrm{K})/T}\ \mathrm{m^2\,s^{-1}}$, and $h_{\mathrm{H}}=h_{\mathrm{D}}=4.05e^{-(4995.3\ \mathrm{K})/T}\ \mathrm{m\,s^{-1}}$.

I. INTRODUCTION

The diffusion of hydrogen isotopes in metals, and in Pd in particular, has been studied extensively using a host of techniques. These studies cover a broad range of interests from the characterization of the H point defect in Pd to mass transport of H in Pd and have been summarized by Völkl and Alefeld[1,2] and by Kehr.[3] Völkl, Alefeld, and co-workers[4] very precisely measured the diffusion coefficients for hydrogen (D_{H}) and deuterium (D_{D}) over the temperature range of 230 to 473 K by Gorsky-effect measurements and demonstrated clearly the inverse isotope effect whereby, at low temperatures, D_{D} is greater than D_{H}. At higher temperatures these values appear to cross as the diffusion coefficient must approach classical behavior in the limit as temperature goes to infinity. Katsuda *et al.*[5] reported very precise values of D_{H} at higher temperatures, using permeation techniques, and Sicking *et al.*[6,7] reported diffusion coefficients for tritium in Pd (D_{T}) near room temperature. The definition of the transition of hydrogen diffusion from a quantum-mechanical process at low temperatures to a classical one at very high temperatures is of considerable theoretical interest, as is the possibility of predicting D_{T} from D_{H} and D_{D}. There is also a wide range of surface effects that may result in discrepancies between gas-solid mass-flow measurements of diffusion and those not involving hydrogen transport across a surface. These effects may result from surface contamination by such common species as CO and S (for example, see Ratajczykowa[8] and Peden *et al.*[9]) or from intrinsic properties of the Pd surface and hydrogen (for example, see Comsa *et al.*[10] and Kay *et al.*[11]).

The present work began as part of the transformation of a simple-expansion pressure-volume-temperature apparatus for measuring the solubilities of hydrogen isotopes in metals[12–14] into one that would continuously dispense hydrogen gas from a known volume while maintaining a constant hydrogen pressure over a metal specimen maintained at constant temperature. Pd was chosen as the metal specimen to test this experimental approach because its hydrogen solubility is well known and not too strongly dependent on temperature,[14] because Pd is less sensitive to surface passivation than most metals, and because a sound sphere of Pd could be fabricated. The assumption of equilibrium across the surface of the Pd allows the boundary-condition concentration to be calculated from the pressure. The relatively minor surface effects support this assumption, and a specimen that was physically and geometrically sound simplifies the solution to Fick's second law. The main experimental challenges of this technique dealt with the discontinuous nature of the diffusion process associated with the more tractable solutions to Fick's second law that are based on the boundary condition changing stepwise at $t=0$ from 0 to some finite value, i.e., very fast valve opening with little overshoot and good pressure control (better than 1%) thereafter. The related discontinuity in the absorption of hydrogen by the specimen is that the initial hydrogen sorption is parabolic in time and has an infinite absorption rate at $t=0$ and at long times has a very slow exponential approach to equilibrium. This paper reports the experimental and analytical approaches to this problem, involving corrections for surface effects near ambient temperatures that yielded precise values for D_{H} and D_{D} over a wide temperature range as well as values for the surface "film" conductance (h) that can be interpreted as the velocity at which H atoms cross the Pd surface. Parameters that may be interpreted as activation energies are reported in units of degrees Kelvin and may be converted to other energy units by taking the product with the gas-law constant in the appropriate units.

II. EXPERIMENT

The Pd sphere used in these experiments was 99.98% pure. It was melted in an aluminum oxide crucible in an UHV all-metal tungsten mesh furnace to produce a casting having a test-tube shape 18 mm in diameter and 40 mm long. This casting was radiographed to determine a region free of voids from which to machine a sphere having a radius of 6.36 mm accurate within 10 μm. The sphere was lapped to be spherical within one part in 5000. The finished sphere was reexamined radiographically for cracks or voids that might compromise it as a macroscopically uniform diffusion medium. The hydrostatic density of the sphere was determined to be 11.990 $\mathrm{Mg\,m^{-3}}$ by liquid immersion weighing compared to 12.00 determined from the Pd x-ray lattice parameter. The Pd sphere weighed 12.948 g yielding a calculated mean radius of 6.364 mm. The H_2 was 99.999% H high-purity gas that was filtered through 200 g of UH_3 powder (1 m^2/g surface area) that had been formed by reacting uranium with the supply gas *in situ*. The D_2 was 99.8% D, 99.999% hydrogen isotopes filtered through UD_3, similar to the H_2.

The ultrahigh-vacuum apparatus for determining the equilibrium constants for hydrogen isotopes in uranium alloys[12,13] and in palladium[14] was used to expand H_2 or D_2 from a known volume ($V1$) with a precision pressure sensor (MKS 94H-1000, 160 kPa f.s.—0.05% accurate) into a volume containing the metal sample ($V2$), calibrated relative to $V1$ for its effective volume as a function of sample temperature. This apparatus was modified by replacing the valve between $V1$ and $V2$ with an automatic pressure control valve (APC, Granville-Phillips Model 216), adding an absolute pressure sensor to $V2$ (MKS 94H-10, 1.6 kPa f.s.—0.05% accurate) for feedback to the APC valve controller, and removing the alumina rod used to reduce $V2$ (Ref. 12) to give better gas conductance between the APC valve and the sample. A differential input voltage, the difference between the output of the $V2$ pressure gauge and a set voltage, to the APC valve controller was used to enhance the performance with respect to instantaneously fixing the pressure over the sample. First, the valve was opened manually at a high rate. As the set point was approached, the valve was switched to automatic and partially closed with manual controls that overrode the automatic controls. At the same time, the gain of the controller was increased by two orders of magnitude. The amount of gas that reacted with the sample is the difference between the moles of gas dispensed from $V1$ and that remaining in $V2$. The pressure-gauge outputs were monitored with 1-mV resolution, 12-V full-scale digital voltmeters that were interfaced to a teletype and paper-type printer that could write at a rate of one measurement per second. Figure 1 shows the pressure response for the pressure sensors on $V1$ and $V2$ during an experiment using a uranium rod 7 mm in diameter by 76 mm long at 1073 K for which the time and pressure responses are typical of the Pd-sphere experiments. The APC-valve opening was typically started at the sound of the teletype. The initial pressure overshoot seldom exceeded 2% of the set point and was rapidly damped out after a few 10-s cycles. The time base was chosen to limit the number of data points collected from the pressure sensor in $V1$ to approximately 1000 and the pressure sensor for $V2$ was not recorded on this time base to simplify data processing, since the high-temperature experiments were over in less than 1 ks and the 25 °C experiments lasted about 1 Ms. The standard

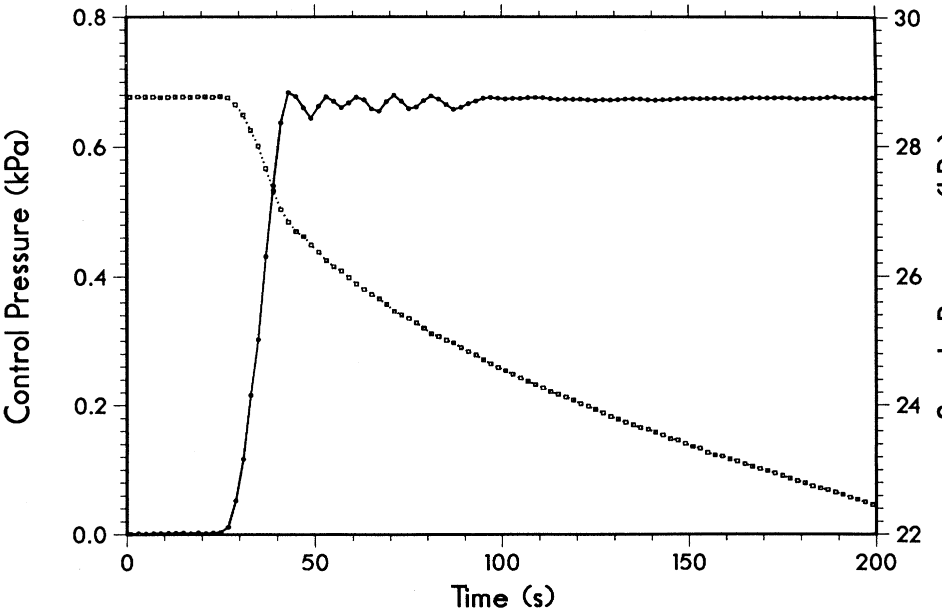

FIG. 1. Typical instrument response for producing a constant pressure over a reacting metal specimen. The solid curve is the control pressure. The dotted curve is the supply pressure. The specimen is a 7-mm-diam, 76-mm-long uranium rod at 1073 K.

deviation of the controlled pressure was typically 0.1% of the setpoint or better over the entire experiment and the set-point pressure was used for calculating the moles of gas in *V*2. Any experiment having an initial overshoot of 5% of the set point or greater was aborted.

After a soap and water wash and rinsing in distilled water followed by absolute ethanol, the Pd sphere was loaded into a 17-mm-internal-diameter aluminum silicate tube with a closed end that was connected to the apparatus by an aluminum silicate-to-Pyrex-to-Kovar-to-stainless-steel seal as part of *V*2. An ungrounded Chromel-Alumel thermocouple mounted in a grounded steel sleeve was placed next to the sphere on the outside of the tube and wrapped with an aluminum silicate sheath inside a quartz cloth-wrapped platinum heat shield mounted within a 1-in. combustion tube furnace. The heat shield extended 75 mm in each direction to ensure a uniform sample temperature, and the temperature-control system with its sensor located in the platinum heat shield maintained the specimen temperature to within 1 K. The sphere was maintained at 1173 K for 10 days while alternately being exposed to 50 kPa H_2 and UHV conditions in one- or two-day cycles. At 473 K and higher temperatures, the experiments were straightforward exercises in setting the temperature, achieving 1 μPa vacuum levels, isolating *V*2, turning on the servovalve, and waiting for equilibrium. Below 473 K, a single experiment required days to acquire the data, after which the sphere was heated to 573 K to facilitate removal of the hydrogen. Once the 1-μPa vacuum was achieved, the specimen was cooled to the appropriate experimental temperature overnight. Most experiments were carried out at 665 Pa H_2 as an optimum level for meeting the conditions of optimum experimental accuracy and dilute hydrogen concentrations (<2 mol% [H]/[Pd] atom ratio). At 298 K, experiments were done at several pressures ranging from 13 Pa to 1.3 kPa to evaluate any concentration dependence of the diffusion process. Care was taken not to expose the Pd sphere to pressures above equilibrium pressures for palladium hydride formation that would probably destroy the physical and geometrical soundness of the sphere. The quantity of H (U, uptake in moles) is shown in Fig. 2 for an experiment at 298 K and 671 Pa H_2. The data were then fitted to mathematical models to determine values for solubility (c_s, $\mathrm{mol\,H\,m^{-3}}$), the diffusion coefficient (D_H, $\mathrm{m^2\,s^{-1}}$), and surface conductance (h_H, $\mathrm{m\,s^{-1}}$).

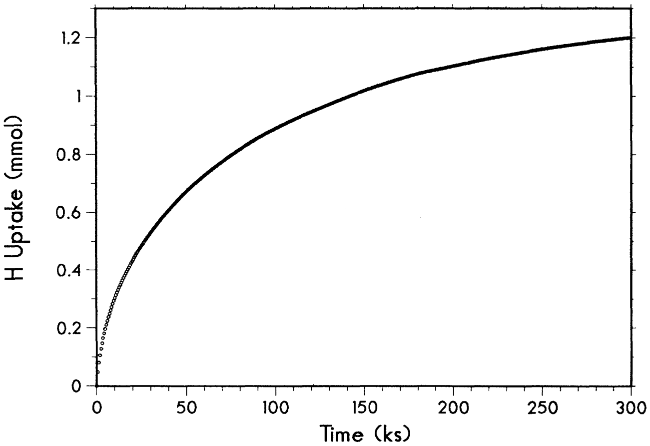

FIG. 2. Hydrogen-uptake data calculated for a 298-K experiment with a control pressure of 1.346 kPa on a Pd sphere (6.36 mm radius). See Run 1 in Table I.

III. MATHEMATICAL FORMULATION OF THE UPTAKE PROBLEM

The uptake problem is one of time-dependent, one-dimensional spherical diffusion. The solution to this problem with no surface conductance is well known and may be found in many references. The solution for the slightly more complicated case, which adds the surface conductance, may be found in, among others, Carslaw and Jaeger.[15] Graphs of the solution to the mathematically equivalent heat transfer problem may be found in numerous places in the conduction heat-transfer literature.[16] The differential equation for the concentration inside the sphere is

$$\frac{\partial c}{\partial t}=D\left[\frac{\partial^2 c}{\partial^2 r}+\frac{2}{r}\frac{\partial c}{\partial r}\right] \quad (0\leq r<a) \tag{1a}$$

with the surface conductance boundary condition

$$D\frac{\partial c}{\partial r}+h(c-c_s)=0 \quad (r=a) \tag{1b}$$

and the initial condition

$$c=0 \quad (t\leq 0)\ , \tag{1c}$$

where c is the concentration of the diffusing hydrogen in the solid metal in units of $\mathrm{mol\,m^{-3}}$, r is the radial coordinate, t is time, D is the diffusivity of the hydrogen atoms in the solid metal in units of $\mathrm{m^2\,s^{-1}}$, h is the surface conductivity in units of $\mathrm{m\,s^{-1}}$, c_s is the solubility of the gas in the metal in units of $\mathrm{mol\,m^{-3}}$ that can be calculated from the hydrogen pressure assuming equilibrium at the surface,[14] and a is the outer radius of the sphere. Equations (1a)–(1c) use a somewhat changed notation from the equations presented in Carslaw and Jaeger, but the mathematical form is the same. The desired result for the present application is not the concentration of the diffusing hydrogen, but rather the total amount of gas absorbed by the solid as a function of time, i.e., the integral of the concentration over the volume of the sphere. We refer to this as the "uptake" with the symbol U.

The units of h are those for velocity, which are rather unusual units for conductance. However, h may be interpreted as a limiting velocity for hydrogen crossing the Pd surface, yielding, when multiplied by c_s, the limiting flux across the Pd surface. An integral form of the surface flux boundary condition, which relates the total rate of uptake to the solubility and surface concentrations, is as follows:

$$\frac{dU}{dt}=4\pi a^2 h(c_s-c)_{r=a}\ . \tag{2}$$

The mathematical problem readily lends itself to nondimensionalization. The nondimensional forms for uptake, time, and surface conductance are as follows:

$$U_{\mathrm{nd}} \equiv U/U_{\mathrm{total}} \ , \tag{3a}$$

$$t_{\mathrm{nd}} \equiv tD/a^2 = N_{\mathrm{Fourier}} \ , \tag{3b}$$

$$h_{\mathrm{nd}} \equiv ha/D = N_{\mathrm{Biot}} \ , \tag{3c}$$

where

$$U_{\mathrm{total}} \equiv \frac{4\pi}{3} a^3 c_s \ . \tag{3d}$$

As noted in Eq. (3b) and (3c), the nondimensional time and surface conductance are the mass transfer equivalents of the Fourier (N_{Fourier}) and Biot (N_{Biot}) numbers which are well-known parameters used to characterize the equivalent problem in the conduction heat-transfer literature. After some algebraic manipulation, the solution to the uptake problem becomes

$$U_{\mathrm{nd}} = 6h_{\mathrm{nd}}^2 \sum_{n=1}^{\infty} [1-\exp(-a_n^2 t_{\mathrm{nd}})] \frac{a_n^2 + (h_{\mathrm{nd}}-1)^2}{a_n^2 + h_{\mathrm{nd}}(h_{\mathrm{nd}}-1)} \frac{1}{a_n^4} \times \sin^2(a_n) \ , \tag{4a}$$

where a_n is the nth root of the following:

$$a_n \cot(a_n) + h_{\mathrm{nd}} - 1 = 0 \ . \tag{4b}$$

In the limit as time approaches zero, the ultimate short-term solution is the integral of Eq. (2) with $c=0$, which may be written in nondimensional form as follows:

$$U_{\mathrm{nd}} = 3h_{\mathrm{nd}} t_{\mathrm{nd}} \ . \tag{5}$$

In the case of a low surface conductance, i.e., $h \rightarrow 0$, the solution to Eq. (1) is

$$U_{\mathrm{nd}} = 1 - \exp(-3h_{\mathrm{nd}} t_{\mathrm{nd}}) \ . \tag{6}$$

In practice, the curve of U_{nd} versus $t_{\mathrm{nd}} h_{\mathrm{nd}}$ for any case which $h_{\mathrm{nd}} < \sim 10^{-2}$ is indistinguishable from that given by Eq. (6). In the case of very high surface conductance, i.e., $h \rightarrow \infty$, the solution to Eq. (1) is

$$U_{\mathrm{nd}} = (6/\pi^2) \sum_{n=1}^{\infty} n^{-2} \{1 - \exp[-(n\pi)^2 t_{\mathrm{nd}}]\} \ . \tag{7}$$

In practice, the curve of U_{nd} versus t_{nd} for any case for which $h_{\mathrm{nd}} > \sim 10^4$ is indistinguishable from one with an infinite surface conductance. In the limit as time approaches zero, the ultimate short-term solution to Eq. (7) may be written

$$U_{\mathrm{nd}} = 6\sqrt{t_{\mathrm{nd}}/\pi} \ . \tag{8}$$

IV. MATCHING THE DATA TO THE MATHEMATICAL MODEL

The curve of uptake versus time, using Eq. (4) from the preceding section is defined with up to four free parameters. The first three are the diffusivity (D), the solubility of hydrogen in the metal (c_s), and the surface conductance (h). The fourth is the initial time (t_0), which represents the initial appearance of the gas. This initial time is not necessarily the same as the zero in the time base for the experimental data. Rather, the zero time is typically assigned as the last data point before a measurable pressure drop in the supply volume $V1$. In effect, for the matching process, the time t in Eq. (4) is replaced by $t - t_0$.

Given t_i, which is the time at which data point i was taken, plus the fit parameters D, c_s, h, and t_0, one may calculate the analytical value of uptake for that time from Eq. (4) (with t replaced by $t_i - t_0$). The best match of the analytic expression to the data is found by minimizing the standard deviation of the data points from the analytic values over the range of possible values of four fit parameters. In other words, one wishes to minimize

$$\sigma \equiv \left[\sum_i \{[U(t_i) - U_i]^2 w_i\} \Big/ \sum_i w_i \right]^{1/2} \ , \tag{9a}$$

where σ is our symbol for the standard deviation, $U(t_i)$ is the calculated uptake from Eq. (4) for time t_i, U_i is the uptake data point at t_i, and w_i is a weighting term for point i. For our standard deviation, we weighted the points by the interval in uptake data, i.e.,

$$w_i \equiv (U_{i+1} - U_{i-1})/2 \ . \tag{9b}$$

The uptake data used for these data-matching computations were those taken after the initial valve opening time and included all data up to 99.5% of the uptake-data maximum.

The estimation of the set of parameters that best fit the data was done using a computer program written by one of the authors (J.R.K.). The program uses the automatic optimizer subroutine U04ECF from the NAG Fortran library. The program will run on either a Cray Research, Inc. X-MP computer or a Digital Equipment Corporation VAX 8650 computer. However, most of the optimization cases in this study were run on the X-MP, which ran many times as fast as the VAX 8650.

V. RESULTS

The results of the matching of the experimental data to the models are given in Table I for hydrogen and Table II for deuterium. Excellent agreement between the surface resistance model and the data is indicated in the U_{nd} standard deviation and, furthermore, the U_{nd} data had little noise at the 0.1% level. The predicted values of c_s using the equations by Lässer and Powell[14,17] agreed with those found by matching, with the standard deviation, of the ratio of these values found to be 2.0% for hydrogen and 1.8% for deuterium. Initial attempts to match the data to the simple diffusion model, Eq. (7),[18] detected the surface resistance problem as the lack of parabolic character at early times for experiments run below 473 K. The problem was dealt with by discarding early time data until a match was obtained. A comparison of the diffusion coefficients and conformance to the model, i.e., the standard deviation of U_{nd}, determined with and without surface conductance, is given in Tables I and II. Figure 3 compares the description of U_{nd} by the two models at early times for a 298-K experiment. Below 473

TABLE I. Results of the matching calculations of the experimental hydrogen uptake data to the diffusion model with and without surface resistance.

Run	Temperature $1/T$ (K^{-1})	Surface conductance h ($m\,s^{-1}$)	Diffusion coefficient with h D ($m^2 s^{-1}$)	Diffusion coefficient without h D ($m^2 s^{-1}$)	Hydrogen solubility Measured c_s (mol H m^{-3})	Hydrogen solubility Calculated c_s (mol H m^{-3})	Control pressure (Pa)	Standard deviation of U_{nd} to the model With h	Standard deviation of U_{nd} to the model Without h
1	0.003 354	2.378×10^{-7}	3.248×10^{-11}	2.850×10^{-11}	1192.0	1218.5	1343.6	0.0008	0.0119
2	0.003 354	2.685×10^{-7}	3.339×10^{-11}	3.100×10^{-11}	797.9	805.9	671.6	0.0007	0.0084
3	0.003 354	1.889×10^{-7}	3.467×10^{-11}	2.952×10^{-11}	102.7	101.5	13.4	0.0012	0.0123
4	0.003 094	6.961×10^{-7}	7.056×10^{-11}	6.363×11^{-11}	247.5	240.8	134.5	0.0004	0.0067
5	0.002 679	5.859×10^{-6}	2.097×10^{-10}	2.042×10^{-10}	350.6	335.1	673.3	0.0002	0.0020
6	0.002 374	1.164×10^{-5}	4.870×10^{-10}	4.706×10^{-10}	246.6	235.7	673.4	0.0002	0.0028
7	0.002 113	1.710×10^{-4}	1.033×10^{-9}	1.028×10^{-9}	181.7	177.8	673.3	0.0003	0.0008
8	0.001 744	6.245×10^{-3}	2.910×10^{-9}	2.905×10^{-9}	124.2	123.9	673.3	0.0003	0.0045
9	0.001 485	1.013×10^{-2}	5.880×10^{-9}	5.872×10^{-9}	98.8	99.0	668.0	0.0005	0.0128
10	0.001 293	4.146×10^{-2}	9.943×10^{-9}	1.046×10^{-8}	86.3	86.1	668.0	0.0031	0.0024
11	0.001 293	4.152×10^{-2}	9.901×10^{-9}	9.907×10^{-9}	85.9	86.1	668.0	0.0005	0.0036
12	0.001 145	7.899×10^{-2}	1.482×10^{-8}	1.474×10^{-8}	79.0	78.8	668.0	0.0007	0.0037
13	0.001 027	8.011×10^{-2}	2.061×10^{-8}	2.129×10^{-8}	74.3	74.5	668.0	0.0006	0.0104
14	0.000 852	1.957×10^{-1}	3.286×10^{-8}	3.312×10^{-8}	70.8	71.4	681.3	0.0005	0.0081
15	0.000 728			4.767×10^{-8}					0.0230

TABLE II. Results of the matching calculations of the experimental deuterium uptake data to the diffusion model with and without surface resistance.

Run	Temperature $1/T$ (K^{-1})	Surface conductance h ($m\,s^{-1}$)	Diffusion coefficient with h D ($m^2 s^{-1}$)	Diffusion coefficient without h D ($m^2 s^{-1}$)	Hydrogen solubility Measured c_s (mol H m^{-3})	Hydrogen solubility Calculated c_s (mol H m^{-3})	Control pressure (Pa)	Standard deviation of U_{nd} to the model With h	Standard deviation of U_{nd} to the model Without h
1	0.003 354	2.421×10^{-7}	4.561×10^{-11}	3.914×10^{-11}	352.2	355.6	684.2	0.0004	0.0163
2	0.003 354	1.683×10^{-7}	4.601×10^{-11}	2.193×10^{-11}	108.4	107.1	67.3	0.0005	0.0152
3	0.003 094	7.979×10^{-7}	8.552×10^{-11}	7.826×10^{-11}	273.1	268.4	673.4	0.0006	0.0086
4	0.002 679	6.921×10^{-6}	2.395×10^{-10}	2.257×10^{-10}	184.2	179.2	673.3	0.0012	0.0020
5	0.002 374	2.614×10^{-6}	5.324×10^{-10}	4.908×10^{-10}	141.6	136.7	673.4	0.0003	0.0284
6	0.002 113	4.466×10^{-5}	1.037×10^{-9}	1.009×10^{-9}	114.8	113.3	706.6	0.0007	0.0017
7	0.001 744	1.647×10^{-3}	2.657×10^{-9}	2.636×10^{-9}	103.5	103.8	999.3	0.0004	0.0006
8	0.001 485	8.462×10^{-4}	4.933×10^{-9}	5.203×10^{-9}	71.4	73.1	668.0	0.0007	0.0095
9	0.001 293	6.169×10^{-3}	8.115×10^{-9}	8.144×10^{-9}	66.6	67.2	668.0	0.0023	0.0060
10	0.001 145	5.084×10^{-2}	1.218×10^{-8}	1.249×10^{-8}	63.4	64.1	668.0	0.009	0.0122
11	0.001 027	3.149×10^{-2}	1.646×10^{-8}	1.653×10^{-8}	62.1	62.7	668.0	0.0006	0.0040
12	0.000 852	1.071×10^{-1}	2.572×10^{-8}	2.619×10^{-8}	62.3	62.6	673.4	0.0010	0.0064
13	0.000 728	1.173×10^{-1}	3.666×10^{-8}	3.661×10^{-8}	63.1	64.5	681.3	0.0381	0.0377

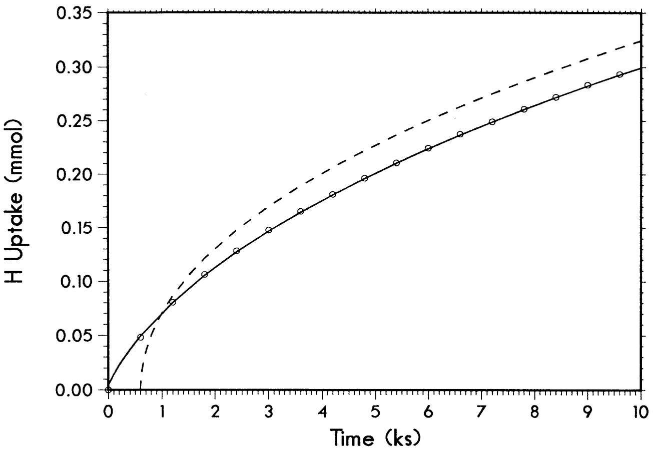

FIG. 3. A comparison of the early-time behavior in terms of the measured data (circles), the surface-conductance model (solid curve) and the diffusion-only model (dashed curve) for the 298-K experiment with a control pressure of 1.346 kPa on a Pd sphere (6.36 mm radius). See Run 1 in Table I.

K, the simple diffusion model overestimated t_0 and meandered back and forth across the experimental data at approximately 100-ks intervals well outside the experimental error yielding low values for D_H and D_D. At these low temperatures, the surface resistance model was essential to a precise description of the data, yielded significantly higher values for D_H and D_D, and yielded values of t_0 within 60 s of the valve opening time. At 473 K and higher temperatures, both models yielded essentially identical values for c_s, D_H, and D_D; values for t_0 that were within the valve opening time and the time between data points was equal to or less than the valve opening time; but the surface conductance model consistently yielded a lower value for the U_{nd} standard deviation.

Figure 4 shows an Arrhenius plot for h. The solid line was determined by linear regression using pooled h data for both hydrogen and deuterium for temperatures at or below 373 K to be

$$h_H = h_D = 4.05e^{-(4995.3\text{ K})/T}\text{ m s}^{-1} . \tag{10}$$

Equation (10) defines the data with standard deviations of 17.2% of its value and 195.6 K for the activation energy below 373 K, where obvious surface conductance effects occur over a long time compared to the valve opening time. Equation (9) also defines the values of h at higher temperatures, where the selection of h may be suspect since the diffusion coefficients could be determined equally well by both models. The lower values for the standard deviation for U_{nd} at the higher temperatures and the "reasonable" values chosen for h for the higher temperatures suggest that the surface conductance significantly affects the overall shape of the uptake curve even at high temperatures. Values for h_{nd} were ~40 at 296 K and approached ~ 10^4 only for temperatures above 1000 K.

Figure 5 shows an Arrhenius plot for D_H and D_D.

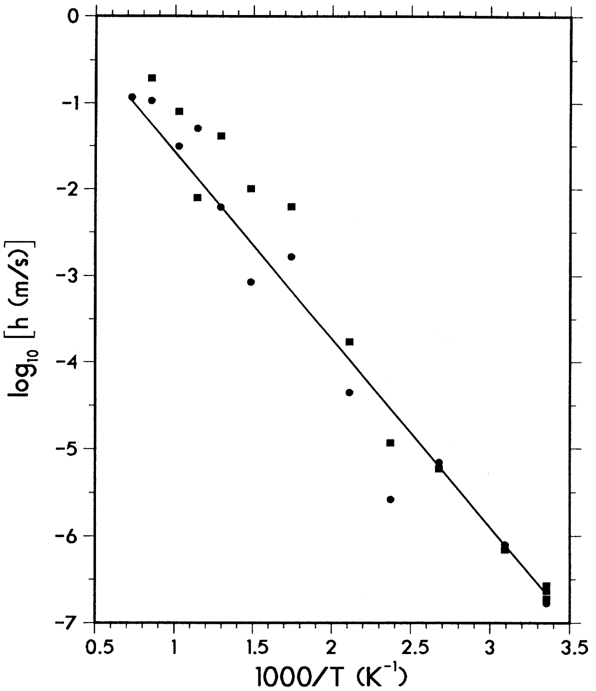

FIG. 4. Surface-conductance measurements obtained from hydrogen (squares) and deuterium (circles) gas-uptake experiments using a Pd sphere (6.36 mm radius). The solid line was determined by matching the pooled H and D data at 373 K and lower temperature to a linear relationship.

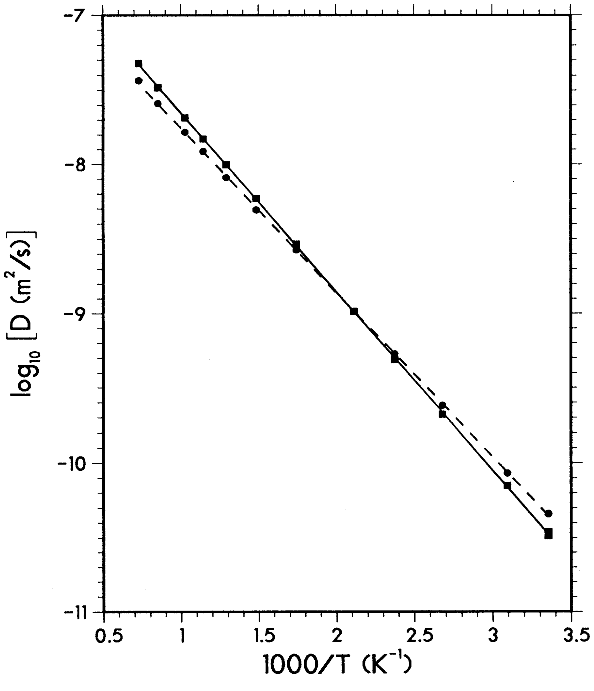

FIG. 5. Diffusion coefficient measurements obtained from hydrogen (squares, solid line) and deuterium (circles, dashed line) gas-uptake experiments using a Pd sphere (6.36 mm radius).

Equations (11) describe D_{H} and D_{D} with standard deviations

$$D_{\mathrm{H}}=3.512\times10^{-7}e^{-(2759.9\ \mathrm{K})/T}\ \mathrm{m}^2\,\mathrm{s}^{-1}\ ,$$
$$D_{\mathrm{D}}=2.219\times10^{-7}e^{-(2538.0\ \mathrm{K})/T}\ \mathrm{m}^2\,\mathrm{s}^{-1}\ , \tag{11}$$

of 2.0% and 2.5% of their respective values and 5.5 and 7.7 K for their respective activation energies. Figure 6 shows good, but not perfect, agreement with other measurements by Völkl *et al.*[4] and Katsuda *et al.*[5] In Fig. 6, data and curves have been rotated by (2600 K)/T to better display their precision. The "inverse-isotope-effect" crossing of D_{H} and D_{D} is well defined with both the coordinate of intersection and the angle of intersection, i.e., the difference between the activation energies of H and D, being the same as that of Völkl *et al.*[4] within experimental error.

The values for D_{H} at 298 K were matched to a linear dependence on c_s for hydrogen and were found to be described by

$$D_{\mathrm{H}}(298\ \mathrm{K})=3.540\times10^{-11}-2.369\times10^{-15}c_s\ \mathrm{m}^2\,\mathrm{s}^{-1} \tag{12}$$

within a standard deviation of 0.42% in estimating D_{H} and 10.6% in the concentration dependence where the concentration is in units of mol H m^{-3}. Equation (12) represents an 8% decrease in the diffusion coefficient over a hydrogen concentration range of 0 to 0.010 57 [H]/[Pd] atom ratio. This concentration dependence is quite small and was not detected by the diffusion-without-surface-conductance model.

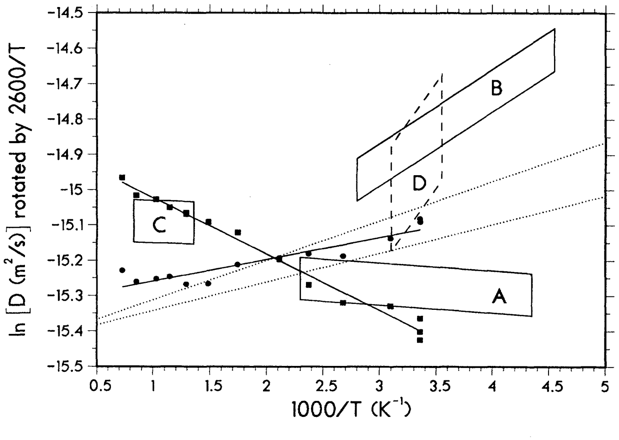

FIG. 6. A comparison of the diffusion coefficients obtained from hydrogen (squares, solid line) and deuterium (circles, solid line) gas uptake experiments using a Pd sphere (6.36 mm radius). All of the data have been rotated by (2600 K)/T to make the relative valves and agreement more apparent. The boxes encompass the experimental error of each experiment. Boxes A and B are the hydrogen and deuterium results of Gorsky-effect measurements by Völkl *et al.* (Ref. 4). Box C is the permeation results for hydrogen by Katsuda *et al.* (Ref. 5). Box D are the tritium permeation results obtained by Sicking *et al.* (Refs. 6 and 7) using electrochemical and tritium tracer techniques. The dotted curves are the predicted range of tritium diffusion coefficients based on the present work.

VI. DISCUSSION

The surface conductance is a significant contributor to the macroscopic transport of H and D in Pd, even when extreme steps have been taken to "clean" the hydrogen gas and the Pd surface. Given the duration of the experiment and the low levels of impurities necessary to effect monolayer coverages of the Pd surface by CO from the residual gas or S segregated to the surface from the Pd bulk, the cleaning process is far from perfect and monolayer quantities of surface impurities may well be present during these experiments. However, the application of the surface resistance model to yield diffusion coefficients, in good agreement with the Gorsky-effect measurements of Völkl *et al.*,[4] measurements independent of surface effects, clearly supports the validity of the modeling. The surface resistance model is derived as a special case of diffusion into two concentric spheres in the limit that the thickness of the outer sphere approaches zero. This outer layer is commonly referred to as a "film" and the surface conductance (h) as the "film coefficient." This lends itself nicely to the interpretation of the surface film as a monolayer-type effect and may be the traplike potential well on the surface or between the first and second Pd monolayers, as described by Comsa *et al.*,[10] Peden *et al.*,[9] I. Ratajcykowa,[8] Kay *et al.*,[11] and Stulen *et al.*[19] Since a diffusion coefficient may be interpreted as the product of a jump distance and a jump velocity, the product of the cube root of the atomic volume of Pd (2.45×10^{-10} m) and the surface conductance yields the diffusion coefficient (D_f) of the "film" given below:

$$D_f=9.92\times10^{-10}e^{-(4995.3\ \mathrm{K})/T}\ \mathrm{m}^2\,\mathrm{s}^{-1}\ . \tag{13}$$

The surface film diffusion coefficient is 350 times smaller than that for bulk Pd at infinite temperature and has an activation energy that is a factor of 1.81 greater than that for H in bulk Pd (1.97 for D) compared with a factor of 2.6 for D given by Comsa *et al.*[10] This would indicate that the surface potential well for Pd is 2457±391 K below the ground state for D in Pd compared with 4172 K given by Comsa *et al.*[10] for the (100) face of single-crystal Pd and 3680 K for H on the (111) surface of Pd given by Engel and Kuipers.[20] Thus the depth of the surface potential is reduced by approximately 1000 K by the peculiar surface conditions of this sample, which includes saturation by hydrogen, and, unless the high hydrogen potential has the effect of displacing CO at six or more orders of magnitude lower potential and reducing segregated S from the surface, CO and S contamination. The lower value for the preexponential part of the D_f is that the "film" coefficient is a velocity derived from a limiting flux using an assumption that the "film" has the same c_s as the bulk. This is almost certainly not the case for a one-monolayer film having a potential twice as deep relative to the diffusion barrier as the bulk. Saturation of the monolayer-type surface film may occur and may be considered as a surface "hydride" phase. Transport of hydrogen across such a "hydride film" no longer resembles impurity diffusion through a host metal, an assumption in the derivation of the model. Another interpretation of the film is that it is a separate metal phase with hydrogen solubility c_s', diffusion coefficient D', and thickness L, such that L is much greater than atomic dimensions yet is negligibly thin compared to the radius a of the sphere. This film can be treated as a slab and, assuming steady-state diffusion of hydrogen through the film is established, the hydrogen flux F is given by

$$F = c_s' D' / L = c_s h \ , \tag{14}$$

where $c_s' D'$ is the permeability coefficient of the film. Equation (14) emphasizes the importance of interpreting the film in terms of the flux of hydrogen across the film, which is rigorously determined as the product $c_s h$. Separation of this flux into a solubility and film coefficient involves assumptions about the nature of the film.

The introduction of the surface resistance model to this problem was to reconcile these data with those of Völkl *et al.*,[4] since within experimental error, they have the same isotope effect and the same values at the crossing point for the "inverse" isotope effect. The surface resistance correction changed the low-temperature diffusion coefficients in the appropriate direction, but not sufficiently to complete the reconciliation that would have given the diffusion coefficient curves a slight positive curvature at low temperatures. At high temperatures, some negative curvature was expected in order for the diffusion coefficients to converge to $D_H / D_D = \sqrt{2}$, the expected classical behavior. The "inverse" isotope effect is well understood[6] in that it is mainly a zero-point-energy effect. If the zero-point energy at the top of the diffusion barrier is greater than that of the ground-state vibrational potential, then the barrier, thus the activation energy, is higher for D than for H. Since H in Pd has a very low vibrational frequency or Einstein temperature ($\Theta_H = 800$ K) relative to most metals,[14] it is not surprising that the saddle point over which the jump occurs may have an Einstein temperature larger than that of the ground state. The inversion, the crossing of the curves for H and D, is imposed by the convergence to classical behavior at very high temperatures. Transition-state theory developed by Vineyard[21] and applied to hydrogen isotope effects by Katz *et al.*[22] and Ebasuzaki *et al.*[23] describe the diffusion coefficient as

$$D = \nu \frac{\Theta^{*2}(1 - c^{-\Theta^*/T})^{-2} e^{-2\Theta^*/2T}}{\Theta^3 (1 - e^{-\Theta/T})^{-3} e^{-3\Theta/2T}} e^{-\varepsilon/T} \tag{15}$$

where ν is proportional to the frequency of the saddle-point crossing, Θ and Θ^* are the Einstein temperatures of the ground state and the transition state normal to the jump direction, respectively ($\Theta_D = \Theta_H/\sqrt{2}$ and $\Theta_T = \Theta_H/\sqrt{3}$, $\nu_D = \nu_H/\sqrt{2}$ and $\nu_T = \nu_H/\sqrt{3}$), and ε is the energy gap between the ground-state vibrational potential minimum and the transition-state vibrational potential minimum. The denominator in Eq. (15) is the vibrational partition function for the ground state of hydrogen in Pd. The results of this treatment applied to the present data are given in Fig. 7. The values $\Theta^* = 1840$ K, $\nu = 1.165 \times 10^{-07}$ cm^2 s^{-1}, and $\varepsilon = 2200$ K were selected to effect the crossing at the appropriate diffusion-coefficient–reciprocal-temperature coordinates. The isotope effect is described very well, but the negative curvature and poor extrapolation to lower temperature result from the assumption of a single value for ν, which implies that transitions from all vibrational energy states are equally probable. This assumption is an obvious oversimplification, but nevertheless, the positive curvature in the Arrhenius plot is inherent in any process whereby the high-energy vibrational states are involved in the diffusion process. Changing the partition function to the more accurate description by Lässer and Powell[14] only exaggerates the positive curvature. The rigorous fit of the data to a constant value of the activation energy strongly argues against a role for the thermal distribution of vibrational energy states in the diffusion process. In order to predict values for tritium, the simple assumptions that the intercept values are proportional to the classical relationship and that the slope, i.e., the activation energy, also scales inversely as the square roots of the relative isotopic masses, as a sole result of zero-point-energy effects, yielded the upper dotted curves in Figs. 6 and 7, having an intersection point with the H data, in common with that for D. Assuming that some phenomena such as the thermal distribution of excited states in transition-state theory compensates for half of this slope effect yields the lower dotted curves in Figs. 6 and 7. These curves are given by

$$D_T = 2.002 \times 10^{-7} e^{-(2503 \pm 15\ \mathrm{K})/T}\ \mathrm{m^2\,s^{-1}} \ . \tag{16}$$

The two dotted curves for T generally represent curves that differ from D by slightly more than twice the experimental error of the D data and embrace the range of predicted intersection angles and coordinates from the models given above. These curves are also consistent with the observations of Sicking *et al.*[6,7] obtained using electrochemical methods.

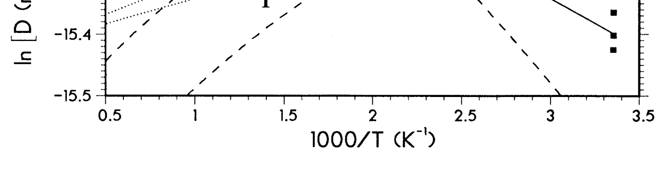

FIG. 7. A comparison of the present results for the diffusion coefficients for hydrogen (squares), deuterium (circles), and tritium (dotted lines) with transition-state-theory predictions (dashed lines). The data have been rotated by (2600 K)/T to make the relative comparison more apparent.

VII. CONCLUSIONS

The uptake of H and D by reaction of pure H_2 and D_2 with the surface of a sound Pd sphere "cleaned" by thermal cycling in the reacting gas is very precisely described by the surface conductance model for diffusion. The surface "film" is consistent with the monolayer trap-like potential at the Pd surface that is a factor of 2 deeper than that of the normal hydrogen site in bulk Pd. Escaping this trap into the bulk of the Pd by diffusion appears to be much less probable than escaping the normal bulk hydrogen site by diffusion. The resulting surface conductance affects the diffusion process even at elevated temperatures. Equations describing the diffusion of H, D, and T in Pd are in general agreement with diffusion coefficients determined by mechanical, electrochemical, and permeation measurements. There appears to be a small concentration dependence on the diffusion coefficient for H in Pd at 298 K.

ACKNOWLEDGMENTS

Oak Ridge Y-12 plant is operated for the U.S. Department of Energy by Martin Marietta Energy Systems, Inc. under Contract No. DE-AC05-84OR21400.

---

[1] J. Völkl and G. Alefeld, in *Diffusion in Solids* (Academic, New York, 1975), Chap. 5, p. 231.

[2] J. Völkl and G. Alefeld, in *Hydrogen in Metals I,* Vol. 28 of *Topics in Applied Physics,* edited by J. Völkl and G. Alefeld (Springer-Verlag, Berlin, 1978), Chap. 12. p. 321.

[3] K. W. Kehr, in *Hydrogen in Metals I* (Ref. 2), Chap. 8, p. 197.

[4] J. Völkl, G. Wollenweber, K.-H. Klatt, and G. Alefeld, Z. Naturforsch. **26A**, 922 (1971).

[5] H. H. Katsuda, R. J. Farraro, and R. B. McClellan, Acta Metall. **27**, 1111 (1979).

[6] G. Sicking, J. Less-Common Met. **101**, 169 (1984).

[7] G. Sicking, M. Gugla, and B. Huber, Ber. Bunsenges. Phys. Chem. **87**, 418 (1983).

[8] I. Ratajcykowa, Surf. Sci. **172**, 691 (1986).

[9] C. H. F. Peden, B. D. Kay, and D. W. Goodman, Surf. Sci. **175**, 215 (1986).

[10] G. Comsa, R. David, and B. Schumacher, Surf. Sci. **95**, L210 (1980).

[11] B. D. Kay, C. H. F. Peden, and D. W. Goodman, Phys. Rev. B **38**, 817 (1986).

[12] G. L. Powell, J. Phys. Chem. **80**, 375 (1976).

[13] G. L. Powell, J. Phys. Chem. **83**, 605 (1979).

[14] R. Lässer and G. L. Powell, Phys. Rev. B **34**, 578 (1986).

[15] H. S. Carslaw and J. C. Jaeger, *Conduction of Heat in Solids,* 2nd ed. (Clarendon, Oxford, 1959).

[16] *Handbook of Heat Transfer Fundamentals,* 2nd ed., edited by W. M. Rohsenow, J. P. Harnett, and E. N. Ganić (McGraw-Hill, New York, 1985).

[17] G. L. Powell and R. Lässer, Z. Phys. Chem. Neue Folge **163**, 47 (1989).

[18] G. L. Powell, R. D. Sharp, and J. S. Tolliver, J. Less-Common Met. **74**, 460 (1980).

[19] R. H. Stulen, T. E. Felter, G. E. Gdowski, and G. D. Kubiak, J. Less Common Metals **64**, 225 (1969).

[20] T. Engel and H. Kuipers, Surf. Sci. **90**, 162 (1979).

[21] G. H. Vineyard, J. Phys. Chem. Solids **3**, 121 (1957).

[22] L. Katz, M. Guinan, and R. J. Borg, Phys. Rev. B **4**, 330 (1971).

[23] Y. Ebisuzaki, W. J. Kass, and M. O'Keefe, J. Chem. Phys. **40**, 1373 (1967).